Resonant oscillations in closed tubes: the solution of Chester's equation

By JAKOB KELLER

Institut für Aerodynamik, Eidgenossiche Technische, Hochschule, Zurich, Switzerland

A closed tube is considered in which the oscillations of a gas column are driven by the sinusoidal motion of a piston. The case where the frequency of the gas column in the tube lies near one of its resonant frequencies is of special interest. The aim of this paper is to extend the theory of Chester (1964), who has given solutions in the inviscid case and for very small boundary-layer friction, to cases of frictional effects of arbitrary strength. This is done by means of a combination of analytical and numerical methods. Different methods are applied for different strengths of the boundary-layer friction. The cases where the influence of the Stokes boundary layer is either very strong or very weak are not especially difficult to treat. The main part of this paper considers cases of intermediate friction, i.e. when the shock strength has grown rather small owing to the influence of the Stokes boundary layer. To obtain an overall view of the phenomena which occur in the different regions, a number of solutions have been calculated.

1. Introduction

This paper discusses the disturbances produced in a closed gas-filled tube by the oscillations of a piston at one end. If the displacement of the piston at time t is $l \sin \omega t$ (where $l \ll L$), acoustic theory says that the particle velocity in the gas is given by

$$u = l\omega \frac{\sin (\omega x/a_0) \cos \omega t}{\sin (\omega L/a_0)},\tag{1}$$

where a_0 is the speed of sound in the undisturbed gas and L the length of the tube. There are certain frequencies where acoustic theory breaks down. Chester (1964) gave a theory for the solution in the frequency band around each resonant frequency, that is when $\sin (\omega L/a_0)$ is near to 0. He developed the equation to solve the problem to second order and gave the solutions in the inviscid case as well as for small effects of boundary-layer friction. In this paper methods are given to solve the problem for boundary-layer effects of arbitrary strength. Chester's analysis uses the following simplifying assumptions.

(i) The Stokes boundary-layer thickness is small compared with the tube radius.

(ii) The Mach number of the flow is small compared with unity everywhere in the tube.

(iii) Terms which arise in the boundary layer can be derived from the linearized boundary-layer equations.

(iv) In the one-dimensional equations describing the mainstream, terms of higher than second order are neglected.

(v) The wall of the tube is kept at constant temperature.

The influence of the boundary-layer effects is taken into account by a convolution integral in the continuity equation.

The first-order equations give a first approximation (u_1, a_1) to the particle velocity and sound speed (u, a), i.e. the acoustic solutions

$$
\left.
\begin{aligned}
u_1 + \frac{2}{\mathscr{H}-1} a_1 &= 2a_0 f\left(t - \frac{x}{a_0}\right), \\
u_1 - \frac{2}{\mathscr{H}-1} a_1 &= 2a_0 g\left(t + \frac{x}{a_0}\right).
\end{aligned}
\right\}
\tag{2}
$$

The suffix '0' refers to values in the undisturbed gas. At one end $(x = 0)$ of the tube there is a rigid barrier, so the first-order boundary condition $u = 0$ at $x = 0$ requires

$$
f = -g.
\tag{3}
$$

A second approximation $(u_1 + u_2, a_1 + a_2)$ is obtained by iteration. The boundary conditions are imposed on this combination of the first- and second-order solutions.

Neglecting effects of compressive viscosity (which are very small in general) this procedure leads to the following equation:

$$
\begin{aligned}
u(x,t) = u_1 + u_2 = a_0 &\left\{ f\left(t - \frac{x}{a_0}\right) - f\left(t + \frac{x}{a_0}\right) \right\} + \frac{\mathscr{H}+1}{4} x \frac{d}{dt} \left\{ f^2\left(t - \frac{x}{a_0}\right) + f^2\left(t + \frac{x}{a_0}\right) \right\} \\
&+ \frac{3-\mathscr{H}}{4} a_0 \frac{d}{dt} \left\{ f\left(t + \frac{x}{a_0}\right) F\left(t - \frac{x}{a_0}\right) - f\left(t - \frac{x}{a_0}\right) F\left(t + \frac{x}{a_0}\right) \right\} \\
&- \frac{\beta x}{2} \int_0^\infty \left\{ f'\left(t - \frac{x}{a_0} - \xi\right) - f'\left(t + \frac{x}{a_0} - \xi\right) \right\} \xi^{-\frac{1}{2}} d\xi \\
&+ \frac{\beta a_0}{4} \int_0^\infty \left\{ f\left(t - \frac{x}{a_0} - \xi\right) + f\left(t + \frac{x}{a_0} - \xi\right) \right\} \xi^{-\frac{1}{2}} d\xi,
\end{aligned}
\tag{4}
$$

where

$$
\frac{d}{dt} F(t) = f(t), \quad \beta = \frac{2}{R}\left(\frac{\nu_0}{\pi}\right)^{\frac{1}{2}} \left\{ 1 + \frac{\mathscr{H}-1}{\mathrm{Pr}^{\frac{1}{2}}} \right\},
\tag{5}
$$

and

$$
\frac{R}{2} = \frac{\text{cross-sectional area of tube}}{\text{perimenter}};
$$

ν, Pr and $\mathscr{H}$ are respectively the coefficient of kinematic viscosity, the Prandtl number and the ratio of specific heats.

The relation (4) for u is now required to satisfy the boundary condition

$$
u = l\omega \cos \omega t \quad \text{at} \quad x = L,
\tag{6}
$$

whereby solutions near resonance are considered, that is when

$$
|\omega L/a_0 - N\pi| \ll 1
\tag{7}
$$

for some integer N. For simplicity, only the case $N = 1$ is considered. It is not difficult to deduce solutions for other values of N.

With the help of (7) we have approximately

$$f\left(t+\frac{L}{a_0}\right) = f\left(t-\frac{L}{a_0}\right) + \frac{2L}{a_0}\frac{\Delta\omega}{\omega}f'\left(t-\frac{L}{a_0}\right),$$

$$f\left(t+\frac{L}{a_0}\right) = f\left(t-\frac{L}{a_0}\right) + \frac{2}{\omega}tg\left(\frac{\omega L}{a_0}\right)f'\left(t-\frac{L}{a_0}\right), \tag{8}$$

where the replacement in the second line is made following Chester, to increase the range of the solution. Equation (3) can now be integrated [by use of (6) and (8)] to give

$$c-\frac{\epsilon}{2}\sin\omega t = \left\{f(t)-\frac{2r}{\pi}\epsilon^{\frac{1}{2}}\right\}^2 - \frac{2\beta}{\mathscr{H}+1}\int_0^\infty f(t-\xi)\,\xi^{-\frac{1}{2}}\,d\xi, \tag{9}$$

where

$$\epsilon = -\frac{4l}{(\mathscr{H}+1)\,L\cos(\omega L/a_0)},$$

$$r = \frac{\pi a_0\,tg(\omega L/a_0)}{(\mathscr{H}+1)\,\omega L\epsilon^{\frac{1}{2}}}, \tag{10}$$

and c is some constant of integration; r will be used as a frequency parameter instead of ω.

Equation (9) will be the basis for the following calculations. Sometimes it is useful to replace f by

$$f(t) = \epsilon^{\frac{1}{2}}g(\lambda), \tag{11}$$

where $\lambda = \omega t$, and to introduce a friction parameter

$$s = \frac{2\beta}{\mathscr{H}+1}\left(\frac{\pi}{\epsilon\omega}\right)^{\frac{1}{2}}, \tag{12}$$

which is essentially the ratio of the boundary-layer thickness to the radius of the tube, divided by the square root of the Mach number of the piston velocity. This is a quotient of two quantities which were assumed to be small.

With the help of (11) and (12), (9) can be rearranged:

$$c-\tfrac{1}{2}\sin\lambda = \{g(\lambda)-2r/\pi^{\frac{1}{2}}\}^2 - (s/\pi^{\frac{1}{2}})\int_0^\infty g(\lambda-\sigma)\,\sigma^{-\frac{1}{2}}\,d\sigma. \tag{13}$$

It can be seen from (13) that g is a function of λ and contains the two parameters r and s:

$$g = g(\lambda; r, s). \tag{14}$$

There is always exactly one solution $g(\lambda; r, s)$ that belongs to a pair of parameters $(r, s \geqslant 0)$. The existence of g is implied physically; the uniqueness follows in the course of the solution from the condition that the mean value of f has to be zero (as required by acoustic theory; this has been shown by Seymour & Mortell 1973) and the fact that discontinuities of rarefaction are forbidden, i.e. the entropy of the system cannot grow smaller.

For the following presentation, it is helpful to mention some important facts about Chester's inviscid solution.

2. The inviscid solution

When the effects of viscosity are ignored, (9) can be written as

$$(f - (2r/\pi)\,\epsilon^{\frac{1}{2}})^2 = \epsilon(B^2 + \cos^2\tau), \tag{15}$$

where

$$2\tau = \omega t + \tfrac{1}{2}\pi, \quad \int_0^\pi f(\tau)\,\mathrm{d}\tau = 0, \tag{16}$$

and B is some constant still to be determined. Now f is required to have zero mean value. The discussion of (15) and (16) together with the definition (10) shows that, if $|r| \geqslant 1$, an appropriate value for B can always be found such that f is continuous and has the same period as the piston; discontinuities are not allowed as long as $|r| \geqslant 1$ because every discontinuity of compression would imply one of rarefaction. If $|r| < 1$, there is no solution as long as B is different from zero. If $B = 0$, there is a unique solution if only discontinuities of compression are admitted. In this case the solution can be written in the form

$$f = \epsilon^{\frac{1}{2}}\{(2r/\pi) \pm \cos\tau\}, \tag{17}$$

and the sign always changes when

$$\sin\tau = r. \tag{18}$$

For $|r| \gg 1$ the acoustic solution is obtained:

$$f = -\epsilon^{\frac{1}{2}}\frac{\pi}{8r}\cos 2\tau = -\frac{\omega l \sin \omega t}{2a_0 \sin(\omega L/a_0)}. \tag{19}$$

In the following sections different methods are developed to solve (9) with the purpose of giving a successful theory in every domain of the r, s plane. As a first step (9) is solved for small values of s.

3. Solution for small values of s

If the evaluation of the convolution integral

$$J_F[f] = -\frac{2\beta}{\mathscr{H}+1}\int_0^\infty f(t-\xi)\,\xi^{-\frac{1}{2}}\,d\xi \tag{20}$$

which occurs in (9) led to a sine and had the same period as the piston oscillation, a solution similar to (17) could be found. The question arises of whether such a replacement can be justified to a certain degree of approximation.

When f is any periodic function with zero mean value, it can be written in the form

$$f(t) = \sum_{\substack{n=-\infty \\ n \neq 0}}^{+\infty} f_n \exp(in\omega t) \equiv \sum_{\substack{n=-\infty \\ n \neq 0}}^{+\infty} c_n^{(0)} \exp(in\omega t); \tag{21}$$

the convolution applied to $f(t)$ gives

$$J_F[f] = -\frac{2\beta}{\mathscr{H}+1}\sum_{\substack{n=-\infty \\ n \neq 0}}^{+\infty}\left(\frac{\pi}{in\omega}\right)^{\frac{1}{2}} f_n \exp(in\omega t) \equiv \sum_{\substack{n=-\infty \\ n \neq 0}}^{+\infty} c_n^{(1)} \exp(in\omega t), \tag{22}$$
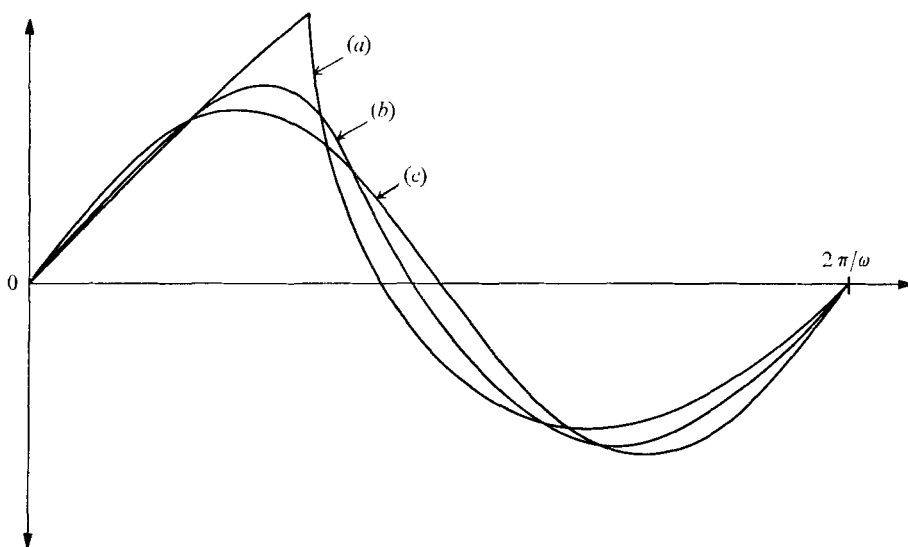
FIGURE 1. Comparison between (a) $J_F[f(t; r = 0, s = 0)]$, (b) $J_F[f(t; r = 1, s = 0)]$ and (c) the corresponding first harmonic, $J_{F1}[f(t; r = 0, s = 0)] = J_{F1}[f(t; r = 1, s = 0)]$.

and when f is convoluted m times,

$$J_F^m[f] = J_F[J_F \dots J_F[f] \dots]$$
$$= \left(\frac{2\beta}{\mathscr{H}+1}\right)^m (-1)^m \sum_{n=-\infty}^{+\infty} \left(\frac{\pi}{in\omega}\right)^{\frac{1}{2}m} f_n \exp(in\omega t) \equiv \sum_{\substack{n=-\infty \\ n \neq 0}}^{+\infty} c_n^{(m)} \exp(in\omega t). \quad (23)$$

Obviously J_F^m approaches a sine asymptotically in the limit $m \to \infty$:

$$\lim_{m \to \infty} \frac{c_n^{(m)}}{c_1^{(m)}} = \begin{cases} 0 & \text{for} \quad n > 1, \\ 1 & \text{for} \quad n = 1. \end{cases} \quad (24)$$

In an iteration procedure when the convolution is repeatedly used, it is seen that the first term is dominant. A comparison between $J[f(t; r = 0, s = 0)]$, $J[f(t; r = 1, s = 0)]$ and the corresponding first Fourier components (see figure 1) shows that a good approximation for f is obtained when $J_F[f]$ is replaced by the first term of its Fourier expansion, i.e.

$$J_{F1}[f] = \frac{\omega}{\pi} \int_0^{2\pi/\omega} J_F[f(\bar{t})] \cos[\omega(t - \bar{t})] \, d\bar{t}. \quad (25)$$

In this case (9) changes to

$$c - \tfrac{1}{2}\epsilon \sin \omega t = \{f_0 - (2r/\pi)\epsilon^{\frac{1}{2}}\}^2 + J_{F1}[f_0]. \quad (26)$$

It will be shown that f_0 is a good basis for a numerical iteration. An appropriate transformation $\mathscr{T}$ converts (26) to

$$\{c + (4/\pi^2)(\epsilon r^2 - \epsilon_0 r_0^2)\} - \tfrac{1}{2}\epsilon_0 \sin(\omega t - 2\tau_0) = \{f_0 - (2r_0/\pi)\epsilon_0^{\frac{1}{2}}\}^2, \quad (27)$$

i.e. f_0 is a 'Chester solution' if we disregard the changed phase angle; f_0 can be written in the form

$$f_0(\tau) = \epsilon_0^{\frac{1}{2}}\{2r_0/\pi \pm \cos(\tau - \tau_0)\} \sim g_0(\lambda), \quad (28)$$

where

$$2\tau = \omega t + \tfrac{1}{2}\pi. \quad (29)$$
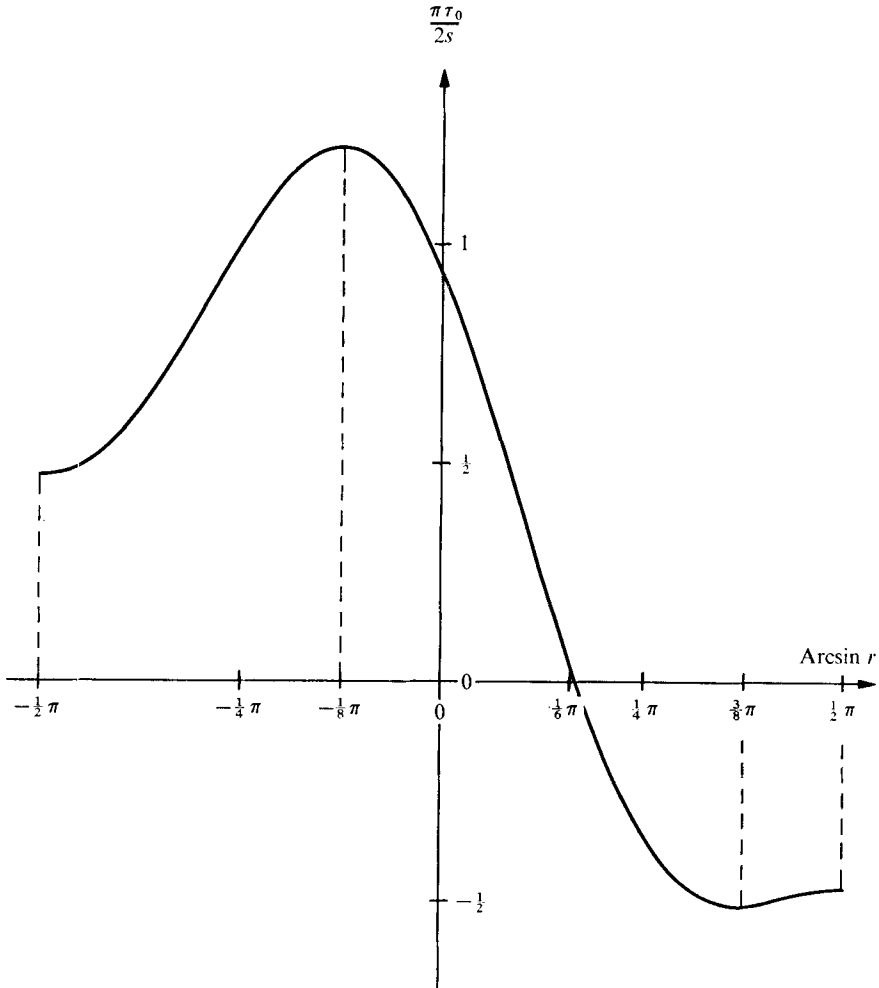
FIGURE 2. The phase angle τ_0 vs. r for small values of s.

The times at which the shocks occur now are given by

$$\tau = \tau_0 + \phi, \tag{30}$$

where, as a consequence of the analogy with Chester's 'inviscid theory',

$$r_0 = \sin \phi. \tag{31}$$

By inserting (28) in (25) J_{F1} is found to be

$$J_{F1} = -2(\epsilon_0/\epsilon)^{\frac{1}{2}} s\{\cos(\omega t - 2\tau_0 - \phi - \tfrac{1}{4}\pi) + \tfrac{1}{3}\cos(\omega t - 2\tau_0 - 3\phi - \tfrac{1}{4}\pi)\}. \tag{32}$$

If this is introduced in (26), a comparison with (27) shows that the transformation $\mathscr{T}$ is given by

$$\epsilon r^2 = \epsilon_0 r_0^2, \tag{33}$$

$$\exp(2i\tau_0) = \left(\frac{r}{r_0}\right)^2 + \frac{r}{r_0}\frac{4}{\pi}s\{\exp(-i(\phi - \tfrac{1}{4}\pi)) + \tfrac{1}{3}\exp(-i(3\phi - \tfrac{1}{4}\pi))\}. \tag{34}$$

This can also be interpreted in the following way: the sum of the piston displacement function and the convolution integral is replaced by a new displacement function. By means of (33) and (34), τ_0 and ϕ can be calculated from r and s; f_0 can be obtained when the new parameters are inserted in (28).

If s is small compared with 1, the imaginary part of (34) can be simplified to

$$\tfrac{1}{2}\pi\frac{\tau_0}{s} = -\{\sin(\phi - \tfrac{1}{4}\pi) + \tfrac{1}{3}\sin(3\phi - \tfrac{1}{4}\pi)\}. \tag{35}$$

With (31), this gives τ_0 as a function of r (see figure 2).

The solution $g_0(\lambda)$ can now be used for an interation. At the nth step the following equation has to be solved:

$$c_n + \left\{g_n(\lambda) - \frac{2r}{\pi}\right\}^2 = -\tfrac{1}{2}\sin\lambda + \frac{s}{\pi^{\frac{1}{2}}}\int_0^\infty g_{n-1}(\lambda - \sigma)\,\sigma^{-\frac{1}{2}}\,d\sigma. \tag{36}$$

Numerical calculations will show (see § 8) that this procedure is convergent as long as $s \lesssim 0.4$; it is used only for values of r for which shocks do occur. The bigger $|r|$ and (or) the smaller s is, the smaller is the difference between $g_0(\lambda)$ and $g(\lambda) = \lim\limits_{n\to\infty} g_n(\lambda)$.

To find the solution for the whole 'shock domain' (that is the part of the r, s plane in which shocks do occur), refined methods will be needed as s increases; the first step will be carried out in the next section. For small values of s, Chester also gave a method of obtaining the solution (taking into account the boundary-layer effects). Indeed, as long as s stays small, the agreement between the results of Chester and the curves given in this paper is very good.

4. Solution for 'intermediate' values of s in the shock domain

The numerical results obtained by means of the methods given in § 3 show that generally the shapes of $g_0(\lambda)$ and $g(\lambda)$ do not differ very much, but a refinement becomes necessary, especially in the neighbourhood of the shocks, when s increases.

4.1. *The signal shape behind the shock*

The higher Fourier components of the convolution integral are responsible for the 'rounding' of the signal shape behind the shock. It will be proved first that the signal f leaves the shock parabolically, i.e.

$$\lim_{\Delta t\to 0}\left\{\frac{f(t_s + \Delta t) - \lim\limits_{t_1\to 0}(f(t_s + t_1))}{(\Delta t)^{\frac{1}{2}}}\right\} \tag{37}$$

exists and is different from zero, assuming that Δt, $t_1 \geqslant 0$. Here t_s is the time co-ordinate at which the shock occurs. The point (r, s) considered lies in the (open) shock domain.

Proof. The signal $f(t)$ can be split into two parts,

$$f(t) = f_1(t) + f_2(t), \tag{38}$$

such that f_1 is a continuous function and

$$f_2(t) = 2k\epsilon^{\frac{1}{2}} \sum_{n=-\infty}^{+\infty} \left\{ \exp\left(-\alpha(t-t_{sn})\right)H(t-t_{sn}) - \frac{1}{\alpha} \right\}, \tag{39}$$

where the strength of the shock (amount of the discontinuous jump) is given by

$$\Delta f_2(t) = 2k\epsilon^{\frac{1}{2}}. \tag{40}$$

Note that f_2 has zero mean value. The times at which the shocks occur are given by

$$t_{sn} = t_s + 2n\pi/\omega, \tag{41}$$

where n is an integer and $t_s = (2\tau_0 + \phi - \frac{1}{2}\pi)/\omega$; $H(t)$ is the Heaviside function defined by

$$H(t) = \begin{cases} 1 & \text{for } t > 0, \\ \frac{1}{2} & \text{for } t = 0, \\ 0 & \text{for } t < 0. \end{cases} \tag{42}$$

The 'damping exponent' α is taken for convenience to be large, i.e.

$$\exp\left(-2\pi\alpha/\omega\right) \ll 1. \tag{43}$$

Notice that $J_F[f] = J_F[f_1] + J_F[f_2]$. A short calculation gives

$$J_F[f_2] \simeq -sk\epsilon \sum_{\substack{n=-\infty \\ n \neq 0}}^{+\infty} \frac{1}{in+\alpha/\omega} \frac{\exp\left(in\omega t\right)}{(in)^{\frac{1}{2}}} = \sum_{\substack{n=-\infty \\ n \neq 0}}^{+\infty} c_n \exp\left(in\omega t\right) \tag{44}$$

$$J_F[f_1] = \sum_{\substack{n=-\infty \\ n \neq 0}}^{+\infty} d_n \exp\left(in\omega t\right).$$

If $n \gg \alpha/\omega$ we have approximately $(in+\alpha\omega)^{-1} \simeq (in)^{-1}$ and therefore

$$c_n \sim n^{-\frac{3}{2}}, \quad d_n = 0, \tag{45}$$

whereby $O(n^{-2})$ is neglected. It can be shown (see §4.2) that the same proportionality appears when the following series is analysed:

$$\sum_{n=-\infty}^{+\infty} (t-t_{sn})^{\frac{1}{2}} \exp\left\{-\alpha(t-t_{sn})\right\} H(t-t_{sn}), \tag{46}$$

where $\alpha \gg \omega$. This is a parabola within some short interval behind every shock. From this it can be seen that

$$\lim_{\Delta t \to 0} \frac{J_F[f(t_s + \Delta t)] - \lim\limits_{t_1 \to 0} J_F[f(t_s + t_1)]}{(\Delta t)^{\frac{1}{2}}} \tag{47}$$

(where $\Delta t, t_1 \geqslant 0$) exists and is different from zero. Equation (9) requires the same behaviour for the quadratic term $(f - 2r\epsilon^{\frac{1}{2}}/\pi)^2$, so that

$$\lim_{\Delta t \to 0} \frac{(f(t_s + \Delta t) - 2r\epsilon^{\frac{1}{2}}/\pi)^2 - \lim\limits_{t_1 \to 0}(f(t_s + t_1) - 2r\epsilon^{\frac{1}{2}}/\pi)^2}{(\Delta t)^{\frac{1}{2}}} \tag{48}$$

(where $\Delta t, t_1 \geqslant 0$) exists and is different from zero. Obviously the relation (37)

follows from this, because if $(f - 2r\epsilon^{\frac{1}{2}}/\pi)^2$ has the property (37), then f has it too, as $f(t_s + 0) - 2r\epsilon^{\frac{1}{2}}/\pi = 0$ is excluded.

For the following calculations the origin of the t axis is changed such that $t = 0$ at a shock. What was called t_s thus far is now set equal to $-t_0$, so that the displacement function in (9) changes to

$$-\tfrac{1}{2}\epsilon \sin \omega(t - t_0).\qquad(49)$$

To analyse the high-frequency components of f the following form of the solution is assumed:

$$f(t) = \sum_{n=0}^{\infty} a_n t^{\frac{1}{2}n},\qquad(50)$$

where $t \geqslant 0$. The derivative of $f(t)$ can be written in the form

$$f'(t) = 2k\epsilon^{\frac{1}{2}} \delta(t) + \tfrac{1}{2}a_1 t^{-\frac{1}{2}} + \Lambda(t),\qquad(51)$$

where $\delta(t)$ is the delta function and $\Lambda(t)$ is defined everywhere. The derivatives (with respect to t) of the convolution integral and the quadratic term in (9) are now given by

$$\frac{d}{dt} J_F[f(t)] = \frac{2\beta}{\mathscr{H}+1} \int_0^\infty f'(t-\xi)\,\xi^{-\frac{1}{2}}\,d\xi = \frac{4\beta}{\mathscr{H}+1} k\epsilon^{\frac{1}{2}} t^{-\frac{1}{2}} + O(1),\qquad(52)$$

$$\frac{d}{dt}\left(f(t) - \frac{2r}{\pi}\epsilon^{\frac{1}{2}}\right)^2 = 2f'(t)\left(f(t) - \frac{2r}{\pi}\epsilon^{\frac{1}{2}}\right)$$
$$= 2(\Lambda(t) + 2k\epsilon^{\frac{1}{2}} \delta(t) + \tfrac{1}{2}a_1 t^{-\frac{1}{2}})\,(k\epsilon^{\frac{1}{2}} + a_1 t^{\frac{1}{2}} + O(t)).\qquad(53)$$

Owing to (9) and the relations (52) and (53) we obtain

$$a_1 = 4\beta/(\mathscr{H}+1).\qquad(54)$$

Note that a_1 does not depend on L, l or ω, i.e. the only geometric variable which has an influence on the 'parabola' in the pressure signal (behind the shock) is the radius of the tube. The coefficient a_1 is essentially the ratio of the boundary-layer thickness and the radius of the tube.

4.2. *Interrelations between the Taylor series and the Fourier series of $f(t)$*

It was seen that on the right-hand side of the origin (i.e. the shock) a Taylor series in powers of $t^{\frac{1}{2}}$ appears. On the left-hand side only integer powers of t occur; this can be seen as follows: the singular points on the time axis (the origin is one of them) are now

$$t_{sn} = n2\pi/\omega.\qquad(55)$$

If the following limit from negative values of t is considered:

$$\lim_{t \to 0} \frac{d^m}{dt^m} J_F[f(t)],\qquad(56)$$

where $m \geqslant 0$, the singularity at the origin is not included in the convolution integral; so this limit exists for arbitrary values of m, i.e. $J_F[f(t)]$ is analytic on

the left-hand side of the origin (supposing that the range considered is small enough). So we write

$$f(t) = \begin{cases} \sum_{n=0}^{\infty} a_n t^{\frac{1}{2}n} & \text{for} \quad 0 \leqslant t \leqslant \Delta t \leqslant 2\pi/\omega, & (57a) \\ \\ \sum_{n=0}^{\infty} b_{2n} t^n & \text{for} \quad 0 \geqslant t \geqslant -\Delta t. & (57b) \end{cases}$$

The sudden change in the Taylor series across the shock is reflected in the high-frequency terms in the Fourier series of f. The function $f(t)$ can be written in the form

$$f(t) = \sum_{n=-N}^{+N} c_n \exp(in\omega t) + \sum_{n=N+1}^{\infty} (c_n \exp(in\omega t) + c_{-n} \exp(-in\omega t)). \quad (58)$$

The first, finite sum is obviously analytic for arbitrary (finite) values of the integer N. To calculate the limit of the Fourier coefficient c_n for $n > N$, an artificial factor $\exp(-\alpha|t|)$ is introduced in (57) and the limit $\alpha \to 0$ is taken in the final result. A short calculation gives

$$c_n \simeq \sum_{k=0}^{\infty} \left(k! \frac{a_{2k} - b_{2k}}{(in\omega)^{k+1}} + \frac{(2k+1)!}{2^{2k+1} k!} \frac{a_{2k+1}}{(in\omega)^{k+\frac{3}{2}}} \right) \quad (59)$$

when $n > N$ and N is large enough. For $k = 0$, the first term corresponds to the jump, and the second to the parabola [see (45)].

4.3. *A refined 'ansatz'*†

The reasons stated above lead to an improved ansatz of the form

$$f(t) = \epsilon_0^{\frac{1}{2}} \left\{ \frac{2r_0}{\pi} + \cos\left(\tfrac{1}{2}\omega t + \phi\right) \right\} - a_0 \exp\left(-\frac{a_1}{a_0} t^{\frac{1}{2}} \right) + b_0 \exp\left(-\gamma\left(\frac{2\pi}{\omega} - t\right) \right), \quad (60)$$

in the interval $0 < t < 2\pi/\omega$. The second term on the right-hand side has the form of $(57a)$ and the third has the form of $(57b)$.

In the first part we still require that

$$\exp\left(-\frac{a_1}{a_0} \left(\frac{2\pi}{\omega}\right)^{\frac{1}{2}} \right) \ll 1, \quad \exp\left(-\frac{2\pi\gamma}{\omega} \right) \ll 1, \quad \left.\begin{array}{c} \\ \\ \end{array}\right\} \quad (61)$$

and that the transformation $(r_0, \epsilon_0) \leftrightarrow (r, \epsilon)$ is given by (34).

As the quadratic term $(f(t) - 2r\epsilon^{\frac{1}{2}}/\pi)^2$ cannot be discontinuous (even at $t = 0$) it follows that

$$a_0 = b_0, \quad (62)$$

and as f has zero mean value, γ is given by

$$2\gamma = (a_1/a_0)^2. \quad (63)$$

Equation (9) will be treated now as a system of equations for Fourier coefficients.

† This word is used for 'trial solution, partly to be justified *a posteriori*'.

The quadratic term and the convolution integral can be written in the form

$$\left(f(t) - \frac{2r}{\pi}\epsilon^{\frac{1}{2}}\right)^2 = \sum_{n=-\infty}^{+\infty} q_n \exp{(in\omega t)}, \tag{64a}$$

$$J_F[f(t)] = \sum_{n=-\infty}^{+\infty} j_n \exp{(in\omega t)}. \tag{64b}$$

When the ansatz (60) is inserted in the left-hand side of (64a) and (64b) the coefficients q_n and j_n are obtained by means of a Fourier analysis. For large values of n we obtain for the leading terms

$$\left.\begin{aligned} q_n &= \frac{\omega}{2\pi} \left\{\frac{D\pi^{\frac{1}{2}} a_1}{(in\omega)^{\frac{3}{2}}} + \frac{a_1^2 + a_0 D(2\gamma - a_1^2/a_0^2)}{(in\omega)^2}\right\} + O(n^{-\frac{5}{2}}), \\ j_n &= -\frac{2\beta}{\mathscr{H}+1} \frac{\omega}{2\pi} \left(\frac{\pi}{in\omega}\right)^{\frac{1}{2}} \left\{\frac{2D}{in\omega} + \frac{1}{2}\pi^{\frac{1}{2}} \frac{a_1}{(in\omega)^{\frac{3}{2}}}\right\} + O(n^{-\frac{5}{2}}), \end{aligned}\right\} \tag{65}$$

where
$$D = \epsilon_0 \cos\phi - a_0. \tag{66}$$

The highest order of n appearing in q_n and j_n is $O(n^{-\frac{3}{2}})$ [see (45)]. As the displacement function of the piston is a sine, it has no influence on a comparison of such terms. A connexion between terms $O(n^{-\frac{3}{2}})$ can be obtained when (65) is inserted in (64), and (64) is introduced in (9); this leads to the relation

$$\lim_{n\to\infty} (n^{\frac{3}{2}} q_n) + \lim_{n\to\infty} (n^{\frac{3}{2}} j_n) = 0, \tag{67}$$

which gives
$$a_1 = 4\beta/(\mathscr{H}+1). \tag{68}$$

This result was obtained previously in a slightly different way [see (54)]. In analogy a comparison of terms $O(n^{-2})$, i.e.

$$\lim_{n\to\infty} \{n^2(q_n - n^{-\frac{3}{2}} \lim_{m\to\infty} (m^{\frac{3}{2}} q_m))\} + \lim_{n\to\infty} \{n^2(j_n - n^{-\frac{3}{2}} \lim_{m\to\infty} (m^{\frac{3}{2}} j_m))\} = 0, \tag{69}$$

gives
$$2\gamma = \left(\frac{a_1}{a_0}\right)^2 \left\{1 - \frac{(1-\frac{1}{4}\pi) a_0}{\epsilon_0^{\frac{1}{2}} \cos\phi - a_0}\right\}. \tag{70}$$

The ansatz (60) has actually not enough degrees of freedom to satisfy the relation (70) because γ is already given by the mean-value condition (63). However, at least for small values of s (when $a_0 \to 0$) the conditions (63) and (70) coincide asymptotically. Thus the condition (67) is valid in the whole open shock domain, but (69) only for $s \to 0$.

The influence of the second and third term on the right-hand side of (60) on the shock strength is still small (in its absolute value) when s becomes comparable to 1; however, when the shock strength has become small, the relative error in the amount of the discontinuous jumps is nevertheless significant, because for numerical methods (see §8) it is especially important to keep this relative error small. We have to take into account the corrections in the shock strength due to the second and third term on the right-hand side of (60) as soon as the considered point (r, s) lies near the edge of the shock domain. The condition
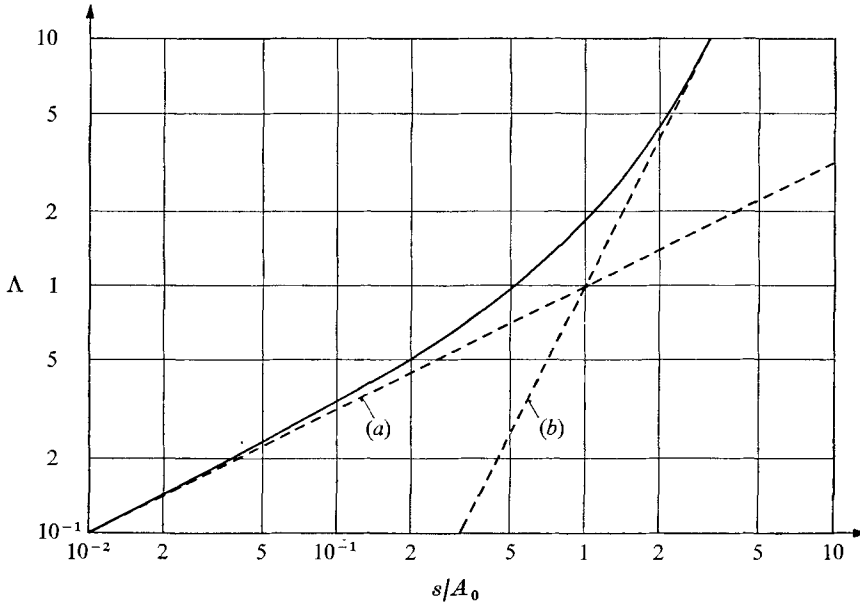
FIGURE 3. A relation between the two exponential functions in the
'refined ansatz'. (a) $\Lambda = (s/A_0)^{\frac{1}{2}}$, (b) $\Lambda = (s/A_0)^2$.

that the quadratic term has to be continuous and the fact that f has zero mean
value give in this case [replacing (62) and (63)]

$$\left(\frac{a_0}{a_1}\right)^2 \mathrm{tgh}\left\{\frac{a_1}{a_0}\left(\frac{\pi}{2\omega}\right)^{\frac{1}{2}}\right\} - \frac{\frac{a_0}{a_1}\left(\frac{2\pi}{\omega}\right)^{\frac{1}{2}}}{1+\exp\left\{\frac{a_1}{a_0}\left(\frac{2\pi}{\omega}\right)^{\frac{1}{2}}\right\}} = \frac{1}{2\gamma}\mathrm{tgh}\left(\frac{\pi\gamma}{\omega}\right), \tag{71}$$

or slightly rearranged (see figure 3)

$$(A_0/s)^2 \mathrm{tgh}\,(s/A_0) - \frac{2A_0/s}{\exp\,(2s/A_0)+1} = \frac{1}{\Lambda}\mathrm{tgh}\,\Lambda, \tag{72}$$

where $A_0 = a_0/(2\epsilon)^{\frac{1}{2}}$ and $\Lambda = \pi\gamma/\omega$. \hfill (73)

Equation (68) has two asymptotes:

$$\Lambda = (s/A_0)^{\frac{1}{2}} \quad \text{when} \quad \Lambda \to 0, \tag{74}$$

and $\Lambda = (s/A_0)^2 \quad \text{when} \quad \Lambda \to \infty,$ \hfill (75)

which agrees with (63). The limit $s \to 0$ corresponds to the second asymptote
(75). The agreement of (63) and (70) gives a measure of the distance between the
actual point $(s/A_0, \Lambda)$ and the asymptote (75) (see figure 3).

For the further discussion of the solutions in the shock domain, numerical
methods are used (see § 8). When s or r becomes large compared with 1, terms of
linear acoustics dominate the solutions and the nonlinear effects can be treated
as a small disturbance.
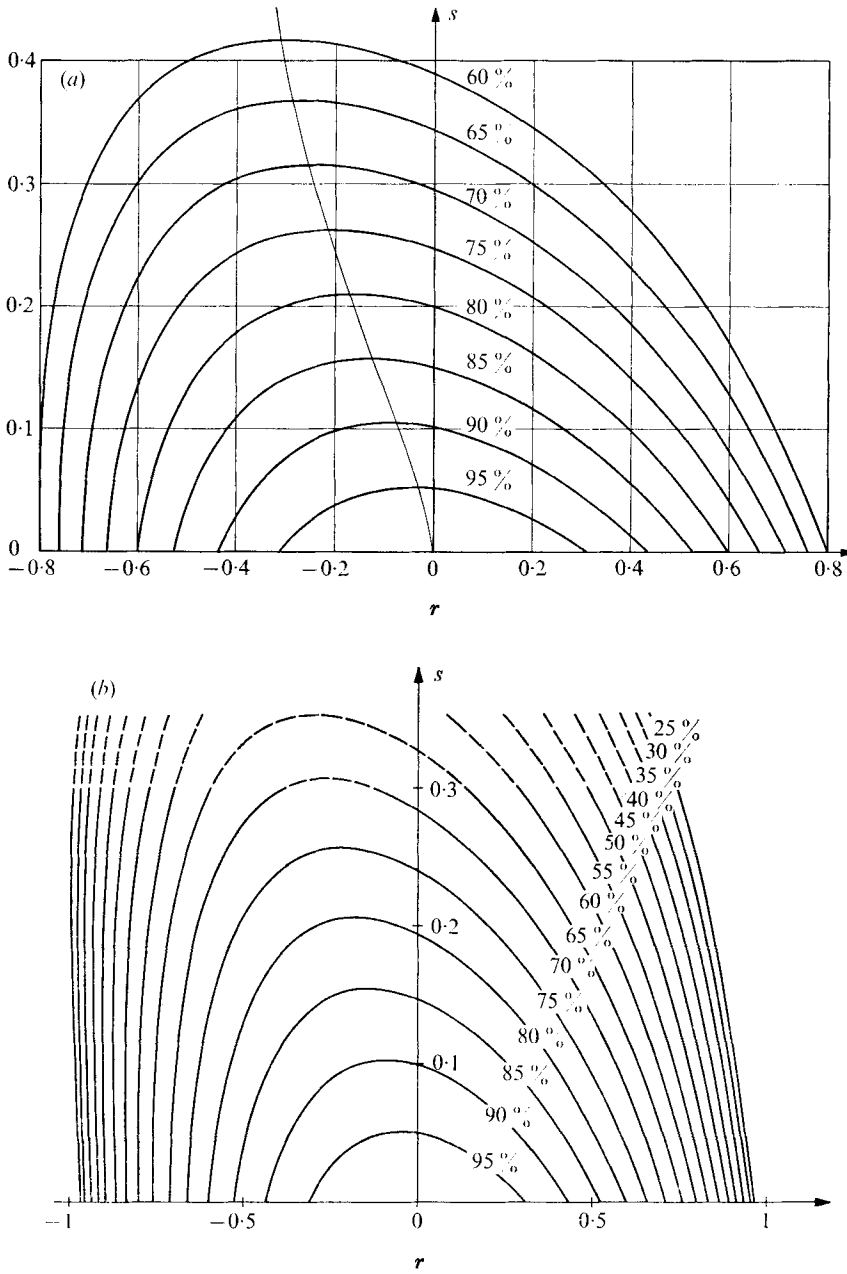
FIGURE 4. Diagram for the shock strength at a fixed value of ϵ calculated (a) by means of a simplified energy method and (b) by means of the energy equation (whereby $J_F[f]$ has been replaced by $J_F[f_0]$).

5. The acoustic domain

With the term f^2 neglected in (9) a problem in linear acoustics is obtained. The elementary solution is

$$f(t) = \epsilon^{\frac{1}{2}} \frac{(2r/\pi)\sin\omega t + \frac{1}{2}s\sin(\omega t + \frac{1}{4}\pi)}{(4r/\pi)^2 + (4\sqrt{2/\pi})\,rs + s^2},$$ (76)

or in standard notation

$$g(\lambda) = \frac{(2r/\pi)\sin\lambda + \frac{1}{2}s\sin(\lambda + \frac{1}{4}\pi)}{(4r/\pi)^2 + (4\sqrt{2/\pi})\,rs + s^2},$$ (77)

and in the special case when $s = 0$,

$$f(t) = (\pi/8r)\,\epsilon^{\frac{1}{2}}\sin\omega t, \quad g(\lambda) = (\pi/8r)\sin\lambda.$$ (78)

The solution (77) is now used as a basis for an iteration, whereby the term $g^2(\lambda)$ is considered as a small disturbance. At the nth step of the iteration the following equation is solved:

$$\{c_{n-1} + g_{n-1}^2(\lambda)\} + \tfrac{1}{2}\sin\lambda = (4r/\pi)\,g_n(\lambda) + s/\pi^{\frac{1}{2}}\int_0^\infty g_n(\lambda - \sigma)\,\sigma^{-\frac{1}{2}}\,d\sigma.$$ (79)

The constant c_{n-1} has to be chosen suitably, i.e.

$$c_{n-1} = -\frac{1}{2\pi}\int_0^{2\pi} g_{n-1}^2(\lambda)\,d\lambda;$$ (80)

so the condition that g should have zero mean value is satisfied.

When the quadratic term is written in the form of a Fourier series

$$c_{n-1} + g_{n-1}^2(\lambda) = h_n(\lambda) = \frac{1}{2}\sum_{\substack{m=-\infty \\ m\neq 0}}^{+\infty}(h_{1n}^{(m)} - ih_{2n}^{(m)})\exp(im\lambda),$$ (81)

g_n can be given as follows:

$$g_n(\lambda) = \frac{(2r/\pi)\sin\lambda + \frac{1}{2}s\sin(\lambda + \frac{1}{4}\pi)}{(4r/\pi)^2 + 4\sqrt{2}\,rs/\pi + s^2}$$

$$+ \sum_{m=1}^\infty \frac{\dfrac{4r}{\pi}\{h_{1n}^{(m)}\cos(m\lambda) + h_{2n}^{(m)}\sin(m\lambda)\} + \dfrac{s}{m^{\frac{1}{2}}}\{h_{1n}^{(m)}\cos(m\lambda + \frac{1}{4}\pi) + h_{2n}^{(m)}\sin(m\lambda + \frac{1}{4}\pi)\}}{\left(\dfrac{4r}{\pi}\right)^2 + \dfrac{4}{\pi}\left(\dfrac{2}{m}\right)^{\frac{1}{2}}rs + \dfrac{s^2}{m}}.$$

(82)

Such an iteration method converges *outside* a certain neighbourhood of $(r = 0, s = 0)$.

6. Summary of methods

At this stage we recall that methods were sought which permit the construction of a solution for any given values $r, s \geqslant 0$. To discuss the applicability of the different methods in the previous sections we use figure 5.

The line C refers to Chester's inviscid theory (see §2). In the domain B, where s is still small, strong shocks occur in the neighbourhood of $r = 0$. The solutions in this domain have been discussed in §3. For the remaining part of the shock
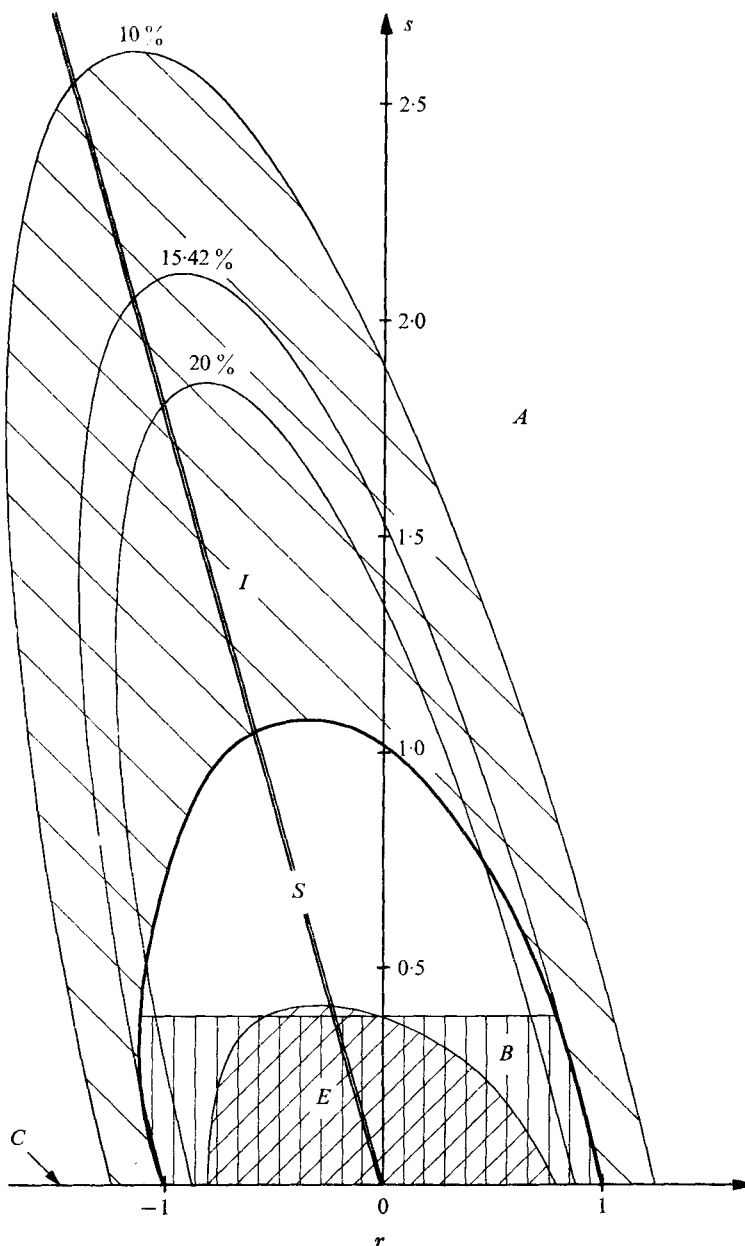
FIGURE 5. Map of all domains considered.

domain S, a method has been developed which is a refinement of the one given in §3 (and naturally also covers the domain B). At the curve which encloses the domain S the shocks just disappear. Beyond this curve the solutions are continuous. Three similar curves are plotted in figure 5; they give the points where the amplitude of the second harmonic of a solution f reaches a certain percentage (10%, $15\cdot42\%$ or 20%) of the amplitude of the first harmonic.

At 15·42 % the curve crosses the points ($r = \pm 1$, $s = 0$). Somewhat beyond this curve the method given in § 5 can be applied. The remaining uncovered part is now entirely contained in the domain *I*. Here solutions can be found with the help of perturbation theory. The calculation may be started from a neighbouring solution or from an analytically iterated acoustic solution. Unfortunately the numerical methods lead to rather lengthy calculations in this domain but on the other hand the shapes of the signals do not vary much here. Thus, if we do not need a very exact solution, we may use an interpolation method. In the domain *E* a simplified method will be given to calculate the strength of the shock (see § 7).

An elementary consideration shows that the amplitude of the acoustic solution $g(\lambda)$ [see (77)] becomes a maximum for a fixed value of *s* when

$$4r/\pi + s/\sqrt{2} = 0. \tag{83}$$

This acoustic resonance line (traced double) is plotted in figure 5; it is an approximate symmetry line for the different domains. (This has already been noticed by Merkli 1973.) The following section gives numerical methods based on the analysis given in the previous sections.

7. The energy balance

7.1. *Simplified calculations of the jumps by an energy method*

When the approximate solution f_0 (see § 3) is inserted in the convolution integral, the error of f_0 is small over the whole period except in a narrow neighbourhood of each shock. Thus we can expect that the integration constant c (obtained by the mean-value condition) in (9) can be set equal to $\tfrac{1}{2}\epsilon_0$ as long as (r, s) is close to $(r = 0, s = 0)$. At $t = 0$ we obtain from (9)

$$\tfrac{1}{2}\epsilon_0 + \tfrac{1}{2}\epsilon \sin \omega t_0 = (\epsilon_0^{\frac{1}{2}} \cos \phi - a_0)^2$$
$$+ \frac{4\beta}{\mathscr{H}+1} \left(\frac{\epsilon_0}{\pi\omega}\right)^{\frac{1}{2}} \sum_{n=1}^{\infty} \left\{\frac{\cos(\phi + \tfrac{1}{4}\pi)}{n^{\frac{1}{2}}(2n-1)} + \frac{\cos(\phi - \tfrac{1}{4}\pi)}{n^{\frac{1}{2}}(2n+1)}\right\}. \tag{84}$$

Alternatively, we could interpret (84) formally as a relation for the energy balance applied to a small interval around a shock co-ordinate. If (27) is considered at the same time,

$$\tfrac{1}{2}(\epsilon_0 + \epsilon \sin \omega t_0) = \epsilon_0 \cos^2 \phi + \frac{4\beta}{\mathscr{H}+1} \left(\frac{\epsilon_0}{\pi\omega}\right)^{\frac{1}{2}} \{\cos(\phi + \tfrac{1}{4}\pi) + \tfrac{1}{3}\cos(\phi - \tfrac{1}{4}\pi)\}, \tag{85}$$

we obtain for the difference between (84) and (85)

$$a_0^2 - 2a_0 \epsilon^{\frac{1}{2}} \cos \phi + \frac{4\beta}{\mathscr{H}+1} \left(\frac{\epsilon_0}{\pi\omega}\right)^{\frac{1}{2}} \{0\cdot912 \cos(\phi + \tfrac{1}{4}\pi) + 0\cdot734 \cos(\phi - \tfrac{1}{4}\pi)\} = 0, \tag{86}$$

using

$$\sum_{n=1}^{\infty} \frac{1}{n^{\frac{1}{2}}} \frac{1}{2n-1} \simeq 1\cdot912, \qquad \sum_{n=1}^{\infty} \frac{1}{n^{\frac{1}{2}}} \frac{1}{2n+1} \simeq 1\cdot067. \tag{87}$$

The magnitude of the shock is given by (40); by means of (60) and (40) it can be written in the form

$$2k\epsilon^{\frac{1}{2}} = 2(\epsilon_1 \cos \phi - a_0). \tag{88}$$

Equations (33), (34) and (86) make it possible to calculate k for any values (r, s), assuming that r and s are small compared with 1 (see figure 4, figure 5, domain E).

When the signals are calculated numerically, the results are often obtained in the form of a Fourier series. In such cases it needs much effort to give an exact value of the shock magnitude. As the energy balance is very sensitive to errors in the magnitude of the jump, it is sometimes useful to apply the energy equation. It will be shown now that this equation can be deduced from (9).

7.2. *The energy equation*

When (9) is differentiated with respect to t, we obtain, after a simple modification,

$$l\omega \cos \omega t = (\mathscr{H}+1) L h'(h - (2r/\pi) \epsilon^{\frac{1}{2}}) - \beta L \int_0^\infty h'(t-\xi) \xi^{-\frac{1}{2}} d\xi, \qquad (89)$$

where $h(t) = f(t - L/a_0)$; the left-hand side is the piston velocity. By means of (2) the pressure at the piston can be given in the form

$$p(t) = 2a_0^2 \rho_0 h(t). \qquad (90)$$

When (89) is multiplied by $-p\omega/2\pi$ and integrated over the period (with respect to t) we obtain

$$-\frac{\omega}{\pi} \rho_0 a_0^2 l\omega \int_{t_s}^{t_s + 2\pi/\omega} h(t) \cos \omega t \, dt = -\frac{\omega}{\pi} \rho_0 a_0^2 (\mathscr{H}+1) L \int_{t_s}^{t_s + 2\pi/\omega}$$

$$\times hh'\left(h - \frac{2r}{\pi} \epsilon^{\frac{1}{2}}\right) dt + \frac{\omega}{\pi} \rho_0 a_0^2 \beta L \int_{t_s}^{t_s + 2\pi/\omega} \int_0^\infty h(t) h'(t-\xi) \xi^{-\frac{1}{2}} d\xi. \quad (91)$$

With the help of (40) the first term on the right-hand side can be integrated to give

$$-\frac{\omega}{\pi} \rho_0 a_0^2 (\mathscr{H}+1) L \int_{t_s}^{t_s + 2\pi/\omega} hh'\left(h - \frac{2r}{\pi} \epsilon^{\frac{1}{2}}\right) dt = \frac{\omega}{\pi} \rho_0 a_0^2 (\mathscr{H}+1) L_{\frac{2}{3}}^2 k^3 \epsilon^{\frac{3}{2}} = \dot{E}_s, \quad (92)$$

where $\dot{E}_s$ is the rate of energy dissipation per unit area of the shock front. The term on the left-hand side of (91) can be interpreted as the rate of energy addition per unit area of the piston. The second term on the right-hand side of (91) gives the rate of energy dissipation per unit cross-section at the walls due to viscous and thermal effects (see appendix). It can be noted that energy considerations, without the use of Chester's equation, were made previously by Betchov (1958) and Temkin (1968). Here, the energy equation is found as a consequence of (9).

To calculate the magnitude of the jumps, the approximate solution f_0 (see § 3) can be inserted in the left-hand-side term and in the second right-hand-side term of (91). By means of (92) it is possible to calculate k. These results (see figure 4 (b)) are valid in about the same domain as the results obtained by the method given in § 7.1 (see figure 4 (a)).

8. Numerical calculations

In this section the computation scheme which leads from the analytical approximate solutions to numerical solutions is sketched.

8.1. *Computation in the domain B*

An approximate solution f_0 can be obtained from (34). This solution is inserted in the convolution integral in (36). With the integration constant c_1 chosen suitably, the minimum of the quadratic term

$$(f_1(t) - (2r/\pi) e^{\frac{1}{2}})^2 \tag{93}$$

becomes zero. At the corresponding t co-ordinate there is a change between the two solutions $f_1^+(t)$ and $f_1^-(t)$ of the quadratic equation [see (36)]. The co-ordinate at which the shock occurs is determined by the condition that f_1 shall have zero mean value; at this point the solution changes again. Now the cycle of iteration is closed.

It is advisable to take into account higher harmonics of the convolution integral successively with the stage of iteration; otherwise, the 'peaks' which occur in $f_n(t)$ would falsify the higher harmonics of $f_{n+1}(t)$ considerably for small values of n. The sequence of points $t_s^{(n)}$ (which refers to the shock co-ordinates) is a sensitive measure of the convergence of this iteration method. To obtain very exact values of the shock strength we may use a linear interpolation method on the left side of the shock, and/or a parabolic interpolation on the right side; we note that convergence of the Fourier series of f is not uniform. The advantage of this method is its simplicity. The general treatment which is given in §4 necessitates more complicated methods.

8.2. *Computation in the domain S*

The ansatz (60) is used as a basis for this method; r_0 or ϕ ($r_0 = \sin \phi$) and ϵ_0 are input parameters which may be chosen arbitrarily. The constant a_1 is known [see (68)]. The fact that the quadratic term in (9) has to be continuous leads to the relation

$$b_0 - a_0 \exp\left(-\frac{a_1}{a_0}\left(\frac{2\pi}{\omega}\right)^{\frac{1}{2}}\right) = a_0 - b_0 \exp\left(-\frac{2\pi\gamma}{\omega}\right). \tag{94}$$

By means of (71), γ can be eliminated and a_0 is the only remaining unknown. The ansatz (60) is inserted in the quadratic term and in the convolution integral, whereby the relation (33) is used. For a given value of a_0 we obtain a piston displacement function. A certain value of a_0 is determined when we require that the amplitudes of the higher harmonics of the piston displacement should be as small as possible. Of course there is some arbitrariness in such an optimization but it has to be noted that the higher harmonics have their minimum at about the same value of a_0. It is proposed to look for the minimum of the geometric mean value. The difference between this (almost sinusoidal) displacement function and its first harmonic is now considered as a small perturbation; it is designated
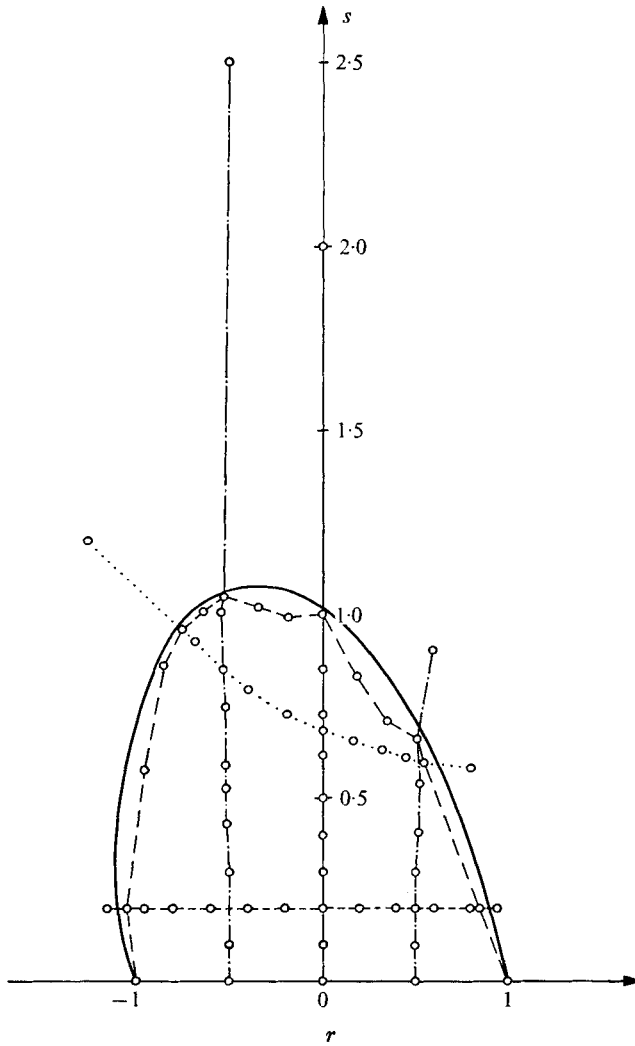
FIGURE 6. Map of the points in the r, s plane referring to the calculated solutions.

by $D[f(t)]$. The difference between the approximate solution $f_u(t)$ [see ansatz (60)] and the exact solution $f(t)$ is called $\Delta f(t)$:

$$f(t) - f_u(t) = \Delta f(t). \tag{95}$$

The corresponding constant of integration is written, in analogy, as

$$c - c_u = \Delta c. \tag{96}$$

When this is inserted in (9) the following relation is obtained:

$$\Delta c + D[\Delta f] = 2\Delta f(f_u - 2re^{\frac{1}{2}}/\pi) + J_F[\Delta f]. \tag{97}$$

This perturbation equation is linear; for the solution it is important to note that

$\Delta f(f_u - 2rc^{\frac{1}{2}}/\pi)$ is a continuous function and $D[\Delta f]$ consists predominantly of low-frequency harmonics; with a suitable choice of a_0, $D[\Delta f]$ almost vanishes. A similar perturbation calculation is used in that part of the domain I where the convergence of the iteration method is bad.

9. Results and discussion

To obtain an overall view, a number of solutions in every domain have been computed. A systematic selection of predetermined pairs (r, s) requires long computing times; the position of the points (r, s) (referring to the computed signals) appears rather arbitrary (see figure 6) but was chosen for convenience, such that the whole plane is covered by computed cases with reasonable density. Six different paths in the r, s plane containing a sequence of points (each) have been chosen to illustrate how $g(\lambda; r, s)$ depends on the parameters (r, s) within a frequency band around the fundamental frequency. In table 1 the values referring to the calculated signals (see also figure 7) are shown. An interesting fact emerges when the magnitude of the shocks $2kc^{\frac{1}{2}}$ is considered as a function of the friction parameter s at $r = 0$. The function $k(s, r = 0)$ has been found to be a straight line (with a very good numerical accuracy):

$$k(s, r = 0) \simeq 1 - s. \tag{98}$$

A comparison with experiments of Saenger & Hudson (1960) shows good agreement. When these theoretical results are compared with experiments of Cruikshank (1972) for small values of s, the same differences appear as in a comparison between these experiments and Chester's theoretical results made by Cruikshank. On the other hand, as was pointed out before, the present theory for small s agrees very well with Chester's results. There must be a fundamental disagreement between Cruikshank's experimental results and Chester's theory; the acoustic symmetry line (83) is contrary to the results of Cruikshank. It was pointed out after (83) that the results of Merkli (1973) agree qualitatively very well with the remarks about this symmetry.

10. Subharmonic nonlinear resonances in closed tubes

It can be seen that (4) has further classes of discontinuous solutions: when the piston is oscillating at one-half of any (odd) resonance frequency, the second-order terms in (4) produce resonant effects. The amplitudes of these 'subharmonic solutions' are $O(M)$. Such a calculation has been carried out by Keller (1975) using the results of the present theory. The inviscid theory shows discontinuous solutions in a bandwidth of the order $\Delta\omega/\omega = O(M)$ around the subharmonic resonance. However, such discontinuities only appear as long as the influence of the boundary layer is very small. The problem of taking into account viscous effects can be solved in the same way as Chester's resonant solutions are treated in the present theory. The results of such a calculation have already been included in Keller (1975). A comparison between that theoretical curve and an experiment

Figure 7 (a)			Figure 7 (b)		
Signal	r	s	Signal	r	s
1	0·500	0·000	1	0·000	0·000
2	0·500	0·100	2	0·012	0·100
3	0·500	0·200	3	0·012	0·200
4	0·500	0·300	4	0·012	0·300
5	0·520	0·403	5	0·018	0·386
6	0·523	0·539	6	0·016	0·496
7	0·512	0·660	7	0·015	0·616
8	0·600	0·900	8	0·014	0·725
			9	0·012	0·847
			10	0·011	0·995
			11	0·020	2·000

Figure 7 (c)			Figure 7 (c) contd		
1	− 0·500	0·000	7	− 0·514	0·588
2	− 0·500	0·100	8	− 0·515	0·746
3	− 0·500	0·200	9	− 0.522	0·845
4	− 0·500	0·300	10	− 0·538	1·005
5	− 0·514	0·430	11	− 0·512	1·047
6	− 0·514	0·526	12	− 0·500	2·500

Figure 7 (d)			Figure 7 (e)		
1	− 1·050	0·200	1	− 0·746	0·959
2	− 0·950	0·200	2	− 0·647	0·927
3	− 0·800	0·200	3	− 0·522	0·845
4	− 0·600	0·200	4	− 0·399	0·794
5	− 0·400	0·200	5	− 0·187	0·727
6	− 0·200	0·200	6	0·009	0·681
7	0·020	0·200	7	0·169	0·653
8	0·200	0·200	8	0·321	0·630
9	0·400	0·200	9	0·451	0·609
10	0·600	0·200	10	0·558	0·592
11	0·800	0·200	11	0·800	0·580
12	0·850	0·200	12	− 1·250	1·200
13	0·950	0·200			
14	− 1·150	0·200			

Figure 7 (f)			Figure 7 (f) contd		
1	1·000	0·000	8	− 0·335	1·019
2	0·850	0·200	9	− 0·512	1·047
3	0·558	0·592	10	− 0·629	1·004
4	0·372	0·709	11	− 0·746	0·959
5	0·194	0·830	12	− 0·846	0·759
6	0·011	0·995	13	− 0·956	0·574
7	− 0·175	0·989	14	− 1·050	0·200
			15	− 1·000	0·000

TABLE 1. Values of r and s for the computed solutions

J. Keller
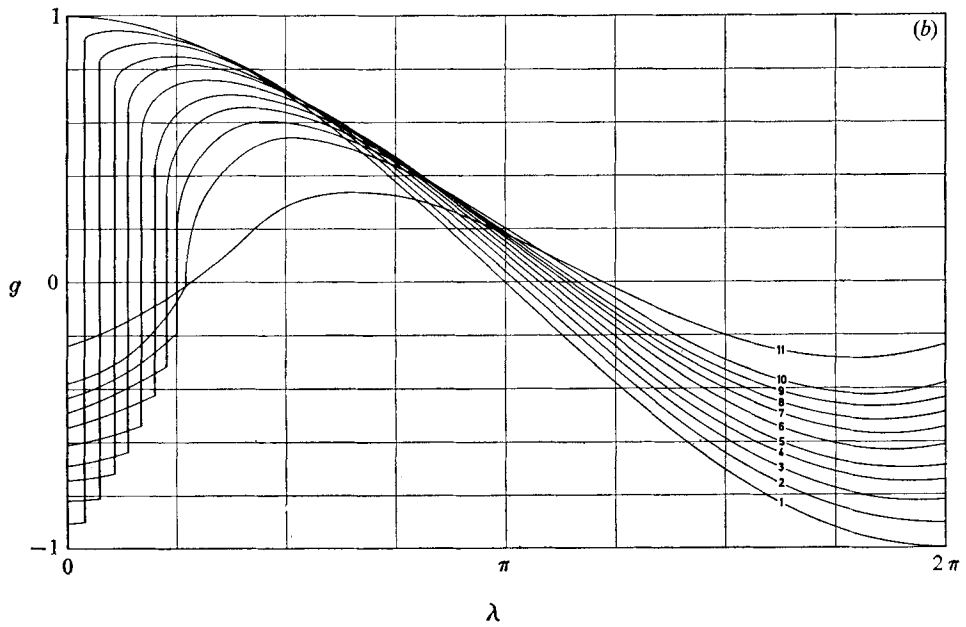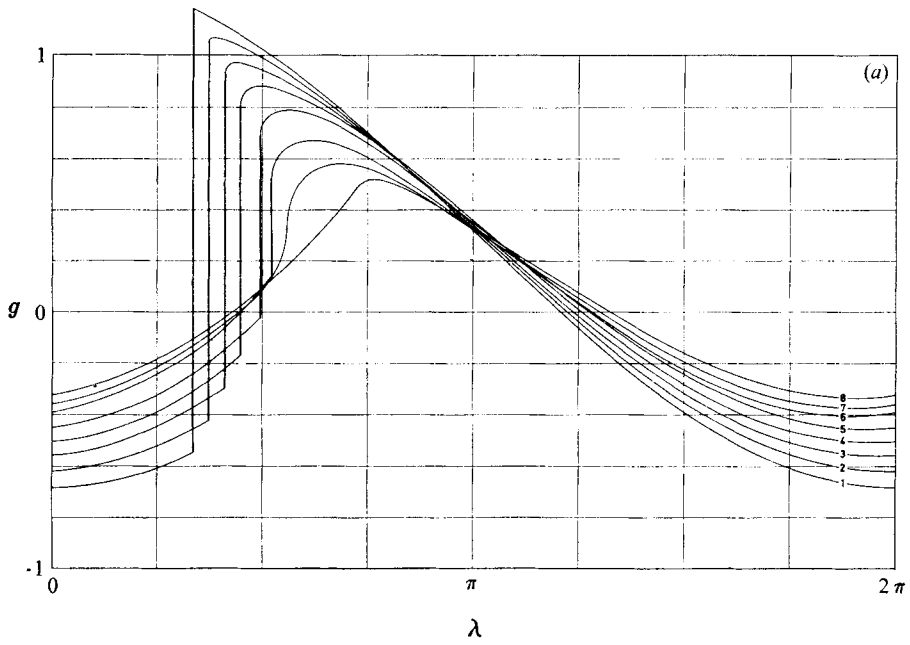
FIGURES 7 (a) and (b). For caption see p. 302.
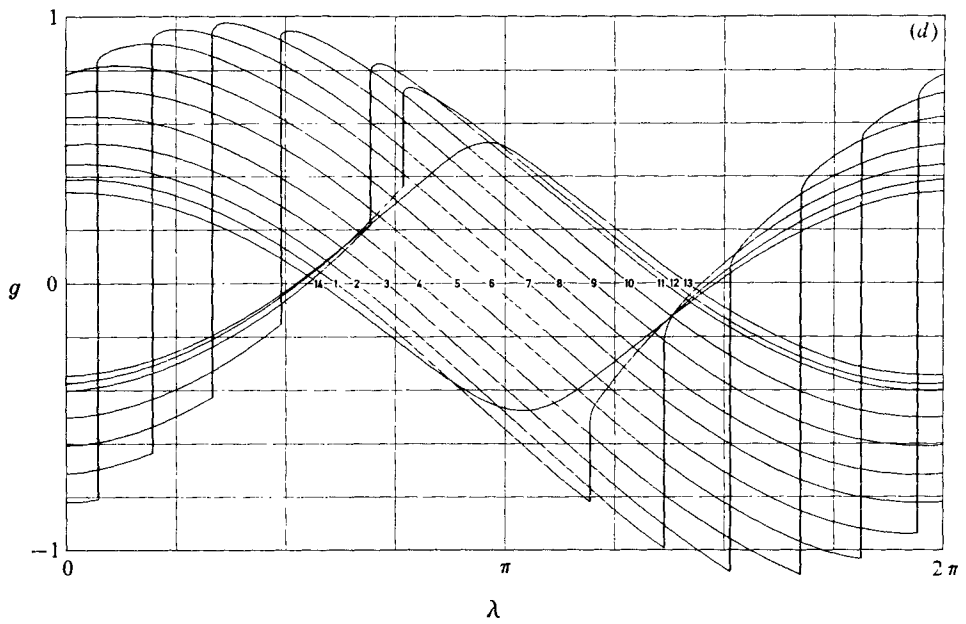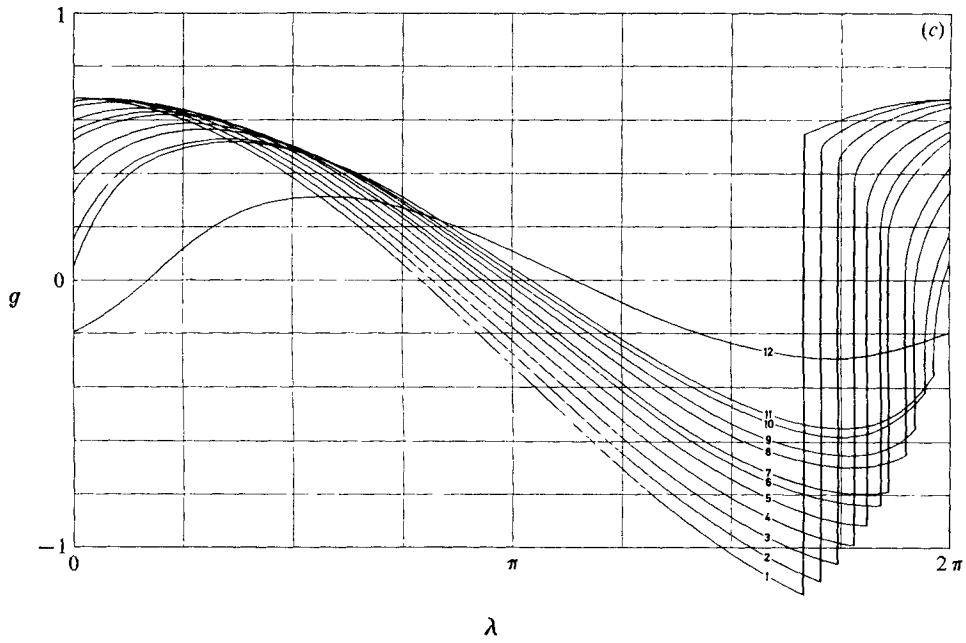
FIGURES 7(c) and (d). For caption see p. 302.

J. Keller
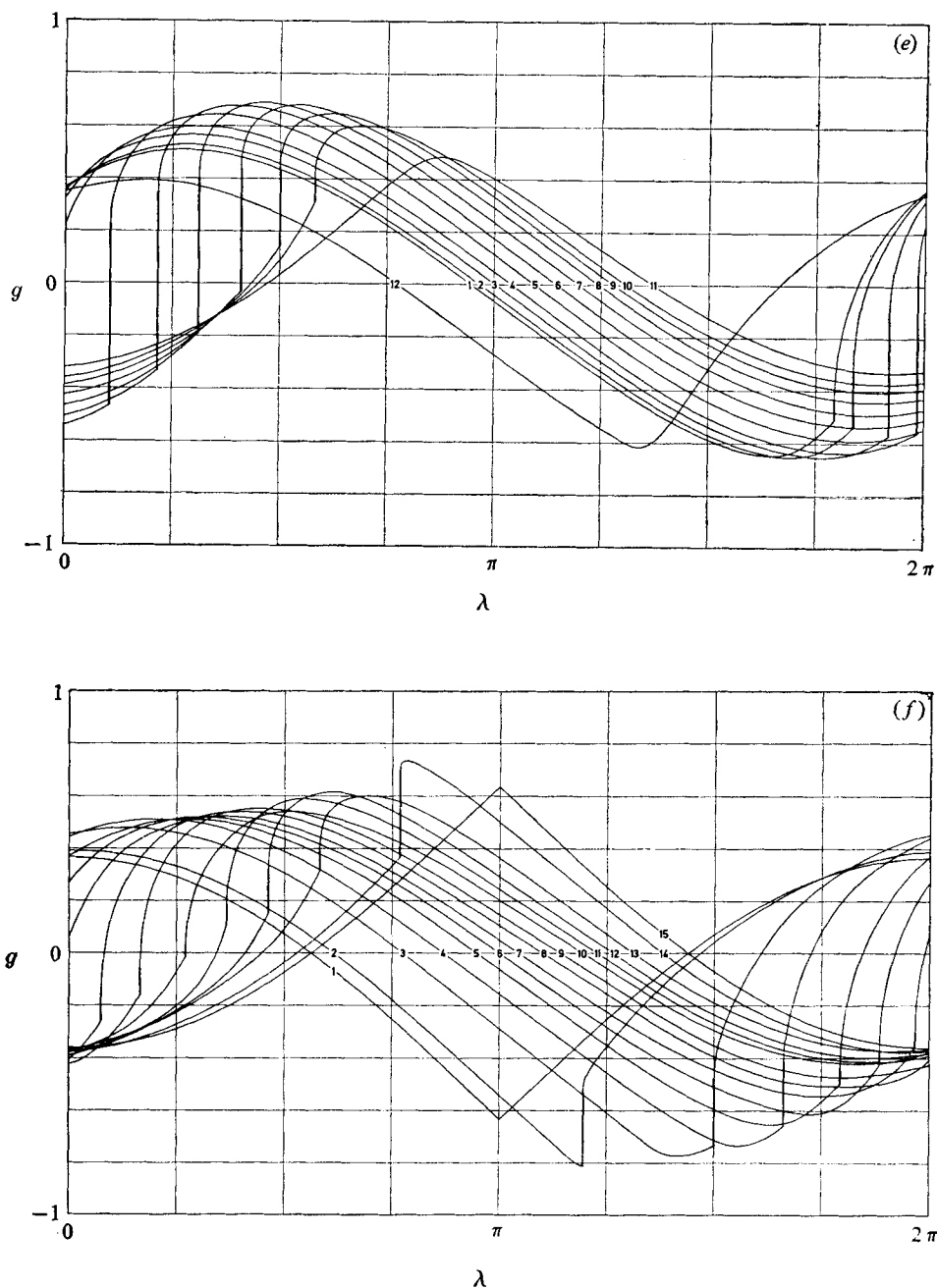
FIGURE 7. The function g *vs.* λ ($= \omega t$) for different values of the parameters (r, s). (a) $r \sim 0.5$; (b) $r \sim 0$; (c) $r \sim -0.5$; (d) $s = 0.2$; (e) intermediate values of s; (f) (r, s) points near the edge of the shock domain.

of Merkli (1973) showed a very good agreement, as far as the shape of the measured pressure signal is concerned; there are no data available that permit a full quantitative check thus far.

This work was prepared as a Ph.D. thesis under the direction of Prof. Nikolaus Rott.

Appendix

The particle velocity in the tube can be written in the form [see (2)]

$$u(x, t) = a_0 \left\{ f\left(t - \frac{x}{a_0}\right) - f\left(t + \frac{x}{a_0}\right) \right\}. \tag{A 1}$$

The velocity in the boundary layer $u_b\,(x, y, t)$ satisfies the following equation:

$$\partial u_b / \partial t = \nu_0 \, \partial^2 u_b / \partial y^2, \tag{A 2}$$

with $u = u_b$ outside the boundary layer and $u_b = 0$ at the wall ($y = 0$). The rate of energy dissipation per unit cross-section of the tube owing to viscous and thermal effects is

$$\dot{E}_w = -\frac{2\mu}{R} \left\{ 1 + \frac{\mathcal{K} - 1}{\mathrm{Pr}^{\frac{1}{2}}} \right\} \frac{\omega}{2\pi} \int_{t_s}^{t_s + 2\pi/\omega} \int_0^L u(x, t) \frac{\partial}{\partial t} u_b(x, y, t)|_{y=0} \, dx \, dt. \tag{A 3}$$

Making use of the boundary conditions (A 2) gives

$$u_b = -u \exp\left(-\left(\frac{\zeta}{\nu_0}\right)^{\frac{1}{2}} y\right); \quad \frac{\partial u_b}{\partial y}\bigg|_{y=0} = \left(\frac{\zeta}{\nu_0}\right)^{\frac{1}{2}} u, \tag{A 4}$$

where ζ is the Heaviside operator. When this is interpreted, we obtain with the help of (A 1)

$$\frac{\partial u_b}{\partial y}\bigg|_{y=0} = \frac{a_0}{(\nu_0 \pi)^{\frac{1}{2}}} \int_0^\infty \left\{ f'\left(t - \frac{x}{a_0} - \xi\right) - f'\left(t + \frac{x}{a_0} - \xi\right) \right\} \xi^{-\frac{1}{2}} \, d\xi. \tag{A 5}$$

Making use of periodic properties of f we can see that

$$\left. \begin{aligned} \int_{t_s}^{t + 2\pi/\omega} \int_0^L f\left(t - \frac{x}{a_0}\right) f'\left(t + \frac{x}{a_0} - \xi\right) dx \, dt &= 0, \\ \int_{t_s}^{t_s + 2\pi/\omega} \int_0^L f\left(t + \frac{x}{a_0}\right) f'\left(t - \frac{x}{a_0} - \xi\right) dx \, dt &= 0, \\ \int_{t_s}^{t_s + 2\pi/\omega} \int_0^L \left\{ f\left(t + \frac{x}{a_0}\right) f'\left(t + \frac{x}{a_0} - \xi\right) + f\left(t - \frac{x}{a_0}\right) f'\left(t - \frac{x}{a_0} - \xi\right) \right\} dx \, dt \\ &= 2L \int_{t_s}^{t_s + 2\pi/\omega} h(t) \, h'(t - \xi) \, dt, \end{aligned} \right\} \tag{A 6}$$

where $h(t) = f(t - L/a_0)$. When (A 5) and (A 1) are inserted in (A 3), we obtain with the help of (5) and (A 6)

$$\dot{E}_w = \rho_0 a_0^2 \frac{\omega L}{\pi} \beta \int_{t_s}^{t_s + 2\pi/\omega} \int_0^\infty h(t) \, h'(t - \xi) \, \xi^{-\frac{1}{2}} \, d\xi. \tag{A 7}$$

REFERENCES

BETCHOV, R. 1958 Nonlinear oscillations of a column of gas. *Phys. Fluids*, **1**, 205.

CHESTER, W. 1964 Resonant oscillations in closed tubes. *J. Fluid Mech.* **18**, 44.

CRUIKSHANK, D. B. 1972 Experimental investigations of finite-amplitude acoustic oscillations in a closed tube. *J. Acoust. Soc. Am.* **52**, 1024.

KELLER, J. 1975 Subharmonic non-linear acoustic resonances in closed tubes. *Z. angew. Math. Phys.* **26**, 395.

MERKLI, P. 1973 Theoretische und experimentelle thermoakustische Untersuchungen am kolbegetriebenen Resonanzrohr. Thesis no. 5151, ETH Zürich.

SAENGER, R. A. & HUDSON, G. E. 1960 Periodic shock waves in resonating gas columns. *J. Acoust. Soc. Am.* **32**, 961.

SEYMOUR, B. R. & MORTELL, M. P. 1973 Resonant acoustic oscillations with damping: small rate theory. *J. Fluid Mech.* **58**, 353.

TEMKIN, S. 1968 Nonlinear oscillations in a resonant tube. *Phys. Fluids*, **11**, 960.